

A GENUINELY MULTIDISCIPLINARY JOURNAL

# CHEMPLUSCHEM

CENTERING ON CHEMISTRY

## Accepted Article

**Title:** Tetrahedral Tetrakis(p-ethynylphenyl)-Group IV-Compounds in Microporous Polymers: Effect of Tetrel on Porosity

**Authors:** Andrea Uptmoor, Florian Geyer, Frank Rominger, Jan Freudenberg, and Uwe Heiko Bunz

This manuscript has been accepted after peer review and appears as an Accepted Article online prior to editing, proofing, and formal publication of the final Version of Record (VoR). This work is currently citable by using the Digital Object Identifier (DOI) given below. The VoR will be published online in Early View as soon as possible and may be different to this Accepted Article as a result of editing. Readers should obtain the VoR from the journal website shown below when it is published to ensure accuracy of information. The authors are responsible for the content of this Accepted Article.

**To be cited as:** *ChemPlusChem* 10.1002/cplu.201800214

**Link to VoR:** <http://dx.doi.org/10.1002/cplu.201800214>

WILEY-VCH

[www.chempluschem.org](http://www.chempluschem.org)

A Journal of



## FULL PAPER

# Tetrahedral Tetrakis(*p*-ethynylphenyl)-Group IV-Compounds in Microporous Polymers: Effect of Tetrel on Porosity

Andrea C. Uptmoor,<sup>[a]</sup> Florian L. Geyer,<sup>[a]</sup> Frank Rominger,<sup>[a]</sup> Jan Freudenberg<sup>[a,b]</sup>\* and Uwe H. F. Bunz<sup>[a,c]</sup>\*

**Abstract:** Three Sonogashira-Hagihara polymerization protocols were applied for the synthesis of conjugated microporous polymers (CMPs) using group IV tetra(*p*-ethynylphenyl) monomers with 1,4-diiodobenzene or 1,4-dibromobenzene. The optical properties and surface areas of the CMPs were compared and related to the preparation conditions and the geometry of the tetrahedral building block as obtained after X-ray analysis. In each series, surface areas decreased - independently from chosen parameters as catalyst, base and solvent - from carbon-centered CMPs (1595 m<sup>2</sup>/g) to silicon-, germanium- and tin-centered (649 m<sup>2</sup>/g) networks.

## Introduction

Rigid tetrahedral building blocks are useful as connectors for the construction of organic porous materials including MOFs,<sup>[1-2]</sup> PAFs,<sup>[3]</sup> COFs<sup>[4-6]</sup> and CMPs.<sup>[7-8]</sup> The latter are formed by irreversible polymerization and applied in gas sorption and separation, as catalyst scaffolding, chemosensors and for energy storage.<sup>[7,9-10]</sup> For amorphous CMPs prepared via Sonogashira-Hagihara coupling, a vast number of synthetic protocols is employed.<sup>[7,11-14]</sup> Differing reaction conditions with respect to catalyst, base, solvent, reaction temperature, nature of the halide and time are reported- and complicate rationalization of fundamental properties like porosity and emission.

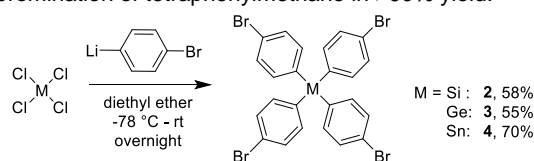
Whereas tetraphenylmethane derivatives have been frequently applied in material sciences,<sup>[15-17]</sup> its silane, germane and stannane congeners were only recently employed to prepare amorphous networks.<sup>[18-19]</sup> Although a few CMPs constructed from tetrahedral carbon and silicon monomers exhibit surface

areas between 717 m<sup>2</sup>/g and 1679 m<sup>2</sup>/g after Sonogashira coupling, the authors again chose differing reaction conditions and started either from tetrahedral tetrahalides or tetraalkynes.<sup>[11,20-21]</sup> There has been no unified investigation of the group IV tetrahedral *p*-ethynylphenyl monomers in Sonogashira-Hagihara polymerizations to date and the influence of the central atom and reaction conditions on the overall properties of the formed CMP has not been systematically investigated.

Previously, we focused on tin-centered microporous polymers and investigated the dependence of optical properties and porosity by varying reaction conditions in Sonogashira-Hagihara couplings of tetrakis(*p*-ethynylphenyl)-stannane with 1,4-diiodobenzene.<sup>[22]</sup> Herein, we disclose scale-optimized syntheses of the four tetrahedral tetraalkynes (C, Si, Ge, Sn) and investigate three Sonogashira-Hagihara coupling protocols for CMP synthesis with 1,4-diiodobenzene or 1,4-dibromobenzene, including change of catalyst, solvent, base and reaction temperature. Although it is not based on Sonogashira coupling, Stefan Kaskel's work (Chem. Commun. 2008. 2462) also can be considered.. We discuss the pronounced central atom effect on the deviation from the perfect tetrahedral shape of the monomers and relate it to the optical properties and surface areas of the CMPs. Although absolute BET areas are highly dependent on the exact reaction conditions, we observe a decrease with increasing atomic number of the central atom for each set of polymers. The term conjugated microporous polymer for this class of materials constructed from tetrahedral *p*-ethynylphenyl compounds of group IV, however, is controversial as we do not know for certain whether the conjugation is limited to the fluorophore embedded between the tetrels or somewhat extends over the central atom (for M = Sn, Ge...) or through-space (vide infra).

## Results and Discussion

The group IV tetrahedral alkynes **9-12** are easily accessible from their tetrabromides **1-4**, which, except for **1**, form from XCl<sub>4</sub> (X = Si, Ge, Sn) and 1-lithio-4-bromobenzene overnight (Scheme 1).<sup>[1,23-26]</sup> Side products are easily removed by crystallization, **2-4** are obtained on multigram scale. Compound **1** is synthesized by bromination of tetraphenylmethane in >90% yield.<sup>[24]</sup>



**Scheme 1.** Synthesis of the tetrabromides **2-4**.

[a] M. Sc. A. C. Uptmoor, Dr. F. L. Geyer, Dr. F. Rominger, Dr. J. Freudenberg, Prof. Dr. U. H. F. Bunz  
Organisch-Chemisches Institut  
Ruprecht-Karls-Universität Heidelberg  
Im Neuenheimer Feld 270  
69120 Heidelberg  
E-mail: [freudenberg@oci.uni-heidelberg.de](mailto:freudenberg@oci.uni-heidelberg.de)  
[uwe.bunz@oci.uni-heidelberg.de](mailto:uwe.bunz@oci.uni-heidelberg.de)

[b] Dr. J. Freudenberg  
Innovation Lab GmbH  
Speyerer Straße 4  
69115 Heidelberg

[c] Prof. Dr. U. H. F. Bunz  
Centre for Advanced Materials  
Ruprecht-Karls-Universität Heidelberg  
Im Neuenheimer Feld 225  
69120 Heidelberg

Supporting information for this article is given via a link at the end of the document.

## FULL PAPER

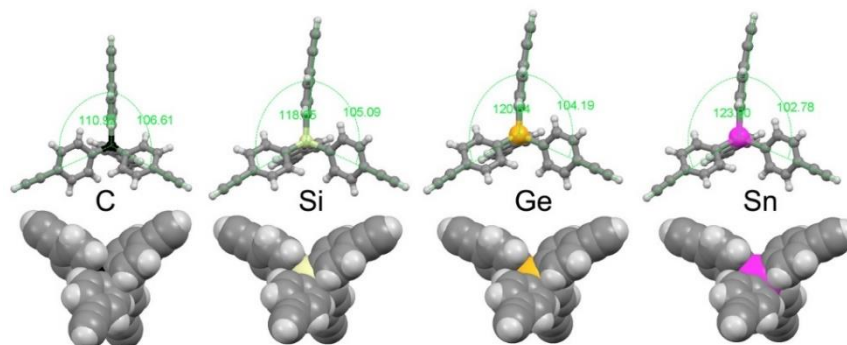
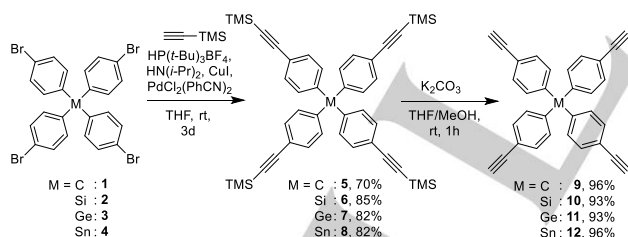


Figure 1. Crystal structures of the alkyne-9-12.

Table 1. Important features of the crystal structures of 9-12.

Alkyne	9	10	11	12
$C_{sp^2}-M_{sp^3}$ -length [Å]	1.55	1.88	1.95	2.14
Arm-length [Å]	6.99	7.31	7.36	7.54
Angles	$4 \times 110.9^\circ$ $2 \times 106.6^\circ$	$4 \times 105.1^\circ$ $2 \times 118.7^\circ$	$4 \times 104.2^\circ$ $2 \times 120.8^\circ$	$4 \times 102.8^\circ$ $2 \times 123.9^\circ$
Average alkyne-alkyne distance [Å]	2.76	2.86	2.87	2.89
Cell axis $a \times b \times c$ [Å]	$12.92 \times 12.92 \times 7.24$	$13.49 \times 13.49 \times 6.70$	$13.60 \times 13.60 \times 6.58$	$13.94 \times 13.94 \times 6.46$
Cell volume [Å <sup>3</sup> ]	1208	1219	1217	1255

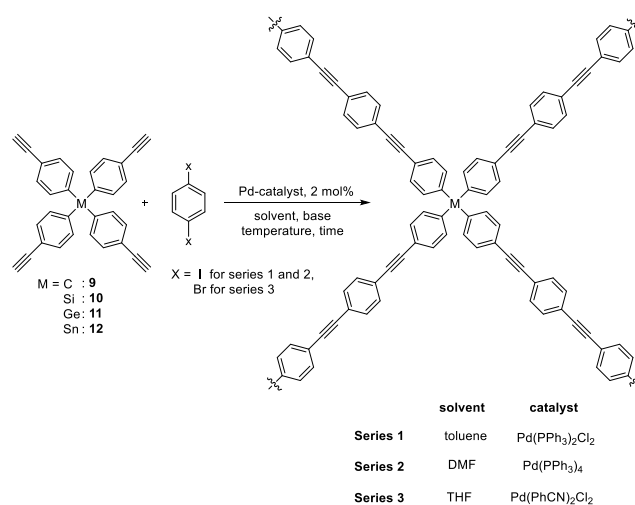
1-4 need an active catalyst system as described by Fu and Buchwald *et al.*<sup>[27]</sup> for the Sonogashira reaction of bromides at room temperature. After 3 d the fourfold reaction forms 5-8 in ca. 80% yield on a scale >3 g. Desilylation ( $K_2CO_3$ ) proceeds almost quantitatively and crystallization from ethyl acetate gives the pure alkyne-9-12 in good to excellent yields (Scheme 2). Crystal structures of 9, 10 and 12 were disclosed recently, but not discussed in context yet.<sup>[26,28-29]</sup> They crystallize in a tetragonal system. Going from carbon to tin, the central atom increases in size and the "arm-length" is increased about 8%, from 9 to 12 (Table 2).<sup>[30]</sup>



Scheme 2. Synthesis of alkyne-9-12.

The compounds crystallize in the  $I\bar{4}$  space group, resulting in a behavior deviating from that of ideal tetraheders because of rising steric freedom. Their cell parameters do not change proportionally to the central atom size: the cell axis  $a$  ( $a=b$ ) grows with the central atom, the  $c$  axis decreases towards 12. Due to the increasing central atom bond lengths an increasing deviation from tetrahedral geometry of the central atom is observed. We synthesized three series following different protocols: i) a procedure we developed recently and tested on tin-centered CMPs (Series 1, CMP C-1-Sn-1),<sup>[22]</sup> ii) a copper-free protocol developed by Thomas *et al.* to avoid alkyne-alkyne-homocoupling

(Series 2, CMP C-2-Sn-2),<sup>[31]</sup> and iii) the literature procedure following Fu *et al.*, which we already used for monomer synthesis, employing 1,4-dibromobenzene instead of its iodide (Series 3, CMP C-3 - Sn-3).<sup>[27]</sup> We modified the literature procedure by adding tris(*tert*-butyl)phosphonium tetrafluoroborate with an excess of base instead of using pyrophoric tris(*tert*-butyl)phosphonium as ligand and changed the solvent from dioxane to THF to ensure good solubility of the monomers. To investigate the influence of the central atom on the surface area and optical properties of porous materials, we synthesized CMPs *via* Sonogashira-Hagihara coupling of 9-12 with 1,4-diiodobenzene or 1,4-dibromobenzene (Scheme 3) and investigated their properties by IR- and optical spectroscopy, TGA-DSC, elemental- and gas sorption analysis.



Scheme 3: Synthesis of the CMPs.

## FULL PAPER

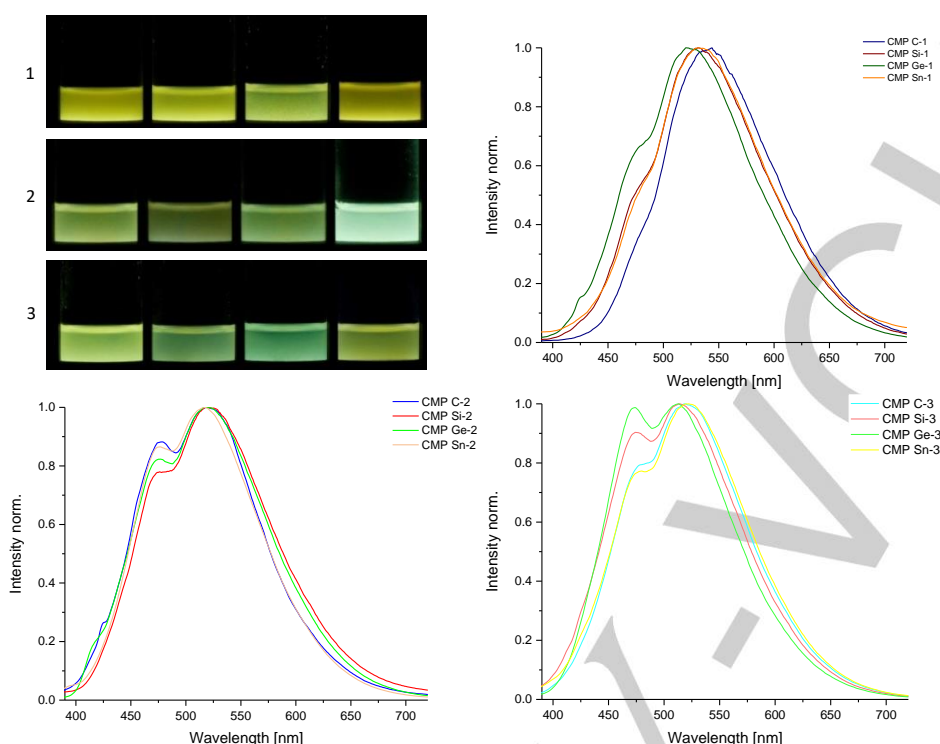


**Figure 2.** Photographs of suspensions of the polymers (THF,  $c = 1 \text{ mg/mL}$ ) under UV-light ( $\lambda = 365 \text{ nm}$ , top left) and emission spectra of the three series.

**Table 2.** Determined emission maxima in the solid state and in suspension for the three polymer series.

CMP Series 1	$\lambda_{\text{em, max}}$ solid state [nm]	$\lambda_{\text{em, max}}$ suspension [nm]	CMP Series 2	$\lambda_{\text{em, max}}$ solid state [nm]	$\lambda_{\text{em, max}}$ suspension [nm]	CMP Series 3	$\lambda_{\text{em, max}}$ solid state [nm]	$\lambda_{\text{em, max}}$ suspension [nm]
C-1	537	544	C-2	527	520	C-3	524	518
Si-1	540	531	Si-2	529	519	Si-3	517	514
Ge-1	535	521	Ge-2	528	517	Ge-3	515	513
Sn-1	543	532	Sn-2	527	517	Sn-3	525	520

The CMPs were obtained as bright yellow to orange powders after Soxhlet extraction from methanol and drying *in vacuo*. They are fluorescent in the solid state as well as in suspension (see Supporting Information).

Whereas CMPs **C-1** to **Sn-1** are brightly yellow fluorescent in suspensions of THF, the other two series exhibit a more greenish emission color (Figure 2). This trend is visible in the emission spectra of the solids and suspensions. The series 1 following our protocol displays fluorescence maxima between 521 nm to 544 nm for suspensions (535 nm and 543 nm in the solid state) whereas the procedure developed by Thomas *et al.* (Series 2) led to maxima lying closely together between 517 nm to 520 nm (527 nm and 529 nm for solid state). The Fu conditions employing 1,4-dibromobenzene (Series 3) resulted in blue-shifted maxima between 513 nm to 520 nm (515 nm and 525 nm in the solid state). Within one series, the emission spectra for the polymers are nearly superimposable. Going from series 1 to 3, however, there

is a second peak at  $\lambda = 470 \text{ nm}$  at higher energies. For series 1, only a small shoulder is apparent, whereas for conditions 2 and 3 the shoulders become distinct peaks. When comparing polymers with the same central atom, emission maxima are shifted about 20 nm to shorter wavelengths when going from conditions 1 to conditions 3 (Figure 2, top right to bottom right). Thus, the choice of the reaction conditions does have an effect on the resulting emission properties. For linear polymers, the position but not the overall shape of emission bands is dependent on the conjugation length, if the effective conjugation length is not reached.<sup>[32-35]</sup> We reason, there is a similar effect at work here, although it is challenging to identify a measure for quantification.

The IR spectra show similar bands for all of the CMPs (see Supporting Information), and there are only weak signals for the terminal alkyne C-H stretching vibration, suggesting high turnover with respect to the alkyne monomers. As emission spectra are more sensitive to the chemical environment of the fluorophores,

## FULL PAPER

small structural differences will impact photoluminescence properties, but will not show up in their IR spectra.<sup>[36-38]</sup>

To investigate whether the central atom influences the porosity of the materials, we determined the BET surface areas by nitrogen adsorption/desorption measurements at 77 K using the BET method. Surface areas vary from 555 m<sup>2</sup>/g for CMP Sn-1 to 1595 m<sup>2</sup>/g for CMP C-2 (Table 2). In all three series, the BET surface areas for the carbon centered CMPs are the highest, whereas the tin centered yielded the lowest -the areas for silicon and germanium are intermediate, but not following the trend. For series 1, the surface area of Si-1 is 55 m<sup>2</sup>/g higher than for Ge-1, but in the other two series, the germanium centered network possesses a somewhat higher surface area. Nonetheless, the values are in a comparable magnitude and can be explained by

the similarity of silicon and germanium (atomic radii etc.), which is also reflected in the structure of the alkyne monomers 10 and 11 (Table 1). Strikingly, the same trend is observed in general, independent from the catalyst system, e.g. solvent, base, precatalyst and dihalide. We hypothesize that this is a direct consequence of the flexibility of the monomers employed as reflected by the increasing deviation from the tetrahedral angle with increasing atomic number and metallic character from carbon to tin (vide supra).

The surface areas in each series could be correlated with the choice of the reaction solvent. Cooper et al investigated solvent changes on the magnitude of the BET areas for a variety of aromatic systems.<sup>[39]</sup>

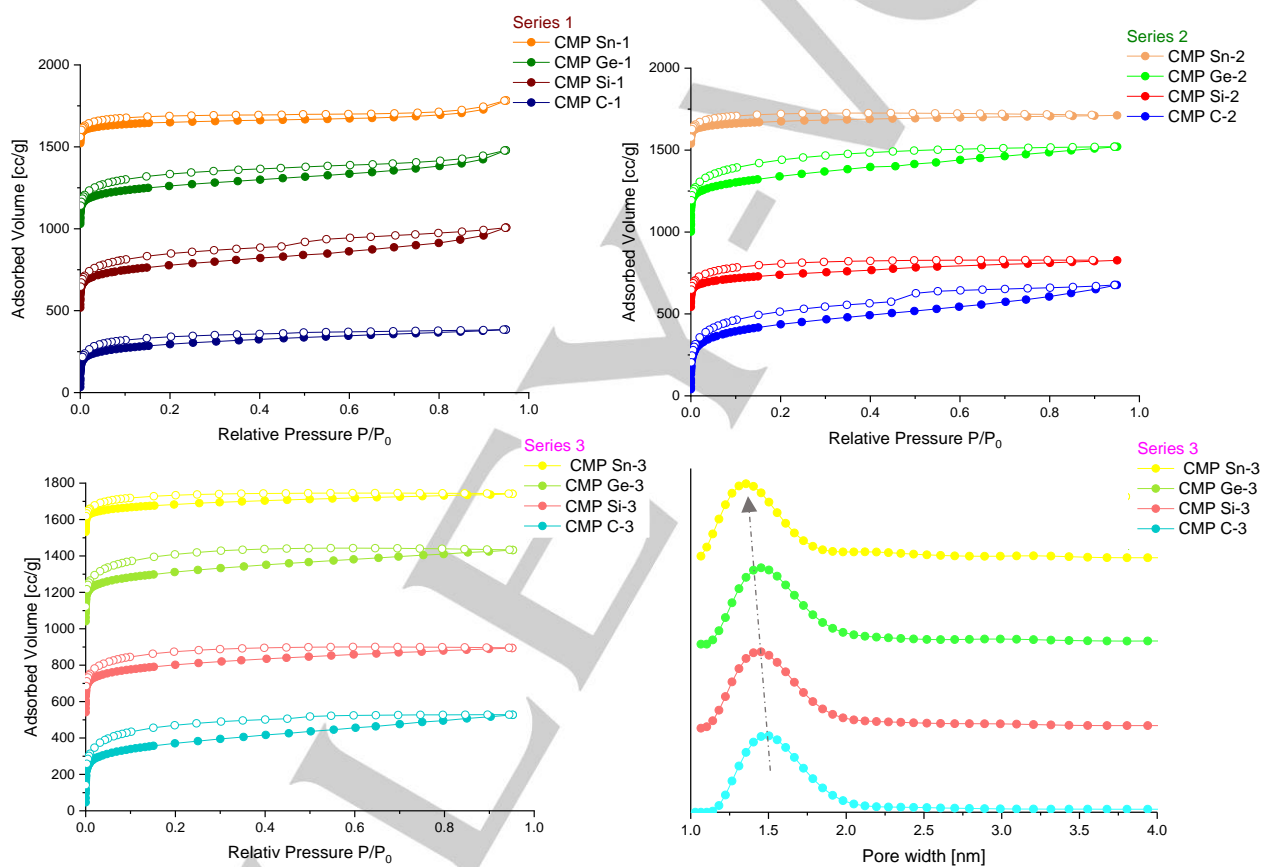


**Figure 3.** Nitrogen adsorption/desorption isotherms (filled symbols = sorption, open symbols = desorption) at 77 K for CMPs **C-1 – Sn-1** (top, left) prepared after our protocol, for CMPs **C-2 – Sn-2** (top, right) prepared after Thomas *et al.* and for CMPs **C-3 – Sn-3** (bottom, left), prepared using Buchwald's and Fu's conditions. The isotherms have been offset by 500 units for clarity. Bottom right: Exemplary progression of the pore size distribution for series 3 (mesopores are not visible in this graph because of their fractional amount).

**Table 3.** Determined surface areas and diameters of the micropores of the three CMP series.

CMP Series 1	BET surface area [m <sup>2</sup> /g]	∅ micropores [nm]	CMP Series 2	BET surface area [m <sup>2</sup> /g]	∅ micropores [nm]	CMP Series 3	BET surface area [m <sup>2</sup> /g]	∅ micropores [nm]
<b>C-1</b>	1086	1.56	<b>C-2</b>	1595	1.73	<b>C-3</b>	1354	1.50
<b>Si-1</b>	1000	1.67	<b>Si-2</b>	1214	1.50	<b>Si-3</b>	1105	1.45
<b>Ge-1</b>	945	1.61	<b>Ge-2</b>	1307	1.61	<b>Ge-3</b>	1132	1.45
<b>Sn-1</b>	555	1.56	<b>Sn-2</b>	649	1.45	<b>Sn-3</b>	667	1.36

## FULL PAPER

The authors tested DMF, THF, dioxane and toluene - DMF always led to the highest surface areas, toluene resulted in least porous networks and THF and dioxane gave intermediate values. This is consistent within our networks. The most rigid carbon-centred monomers, least deformable, result in more rigid and porous, amorphous networks. The N<sub>2</sub>-isotherms (Figure 3) show an apparent hysteresis upon desorption, consistent with the existence of a small amount of mesopores within the polymeric structure.<sup>[11]</sup> The pore size distribution calculated from quenched solid state density functional theory (QS-DFT) affirms this statement as it reveals pores in the mesoporous region ranging from 2.99 nm to 4.08 nm (see Supporting Information) as well as micropores ranging from 1.36 nm to 1.73 nm (Table 3). Cavities for carbon centered polymers are largest and decrease towards the tin centered ones (Figure 3, bottom right). Concerning their micropores, the behavior of silicon and germanium centered networks relates to the determined surface areas: A higher surface area goes hand in hand with larger micropores.

## Conclusions

In conclusion, we present scalable syntheses for the chemically and thermally stable tetrahedral alkyne building blocks **9-12**. With the central atom, some important molecular properties like size (and thus pore-volume, surface area and diameter of derived materials), accessibility of the central atom and flexibility are systematically varied, while others (space group, stability) remain constant. We synthesized three series of conjugated microporous polymers under three different conditions, varying catalyst system, solvent and base as well as the employed dihalide. We compared their optical properties and determined BET surface areas. The emission maxima only change by a few nanometers, but there is a second peak forming in the blueshifted region when changing the reaction conditions from series 1 to series 3. The observed surface areas strikingly differ: We acquired fairly high surface areas for this class of materials (up to 1595 m<sup>2</sup>/g) and determined that within the group IV, the surface area decreases from carbon to tin, irrespectively of the selected conditions for preparation, with the Thomas system giving the highest microporosities. This observation matches with previous investigations about the absolute dimension of surface areas, depending on the choice of the reaction solvent.<sup>[39]</sup> In general, the surface areas of microporous polymers constructed from the group IV tetrahedral alkyne monomers with 1,4-diiodobenzene showed a decreasing trend with increasing atomic number of the central atom.

## Experimental Section

**Materials and Methods.** Unless otherwise described, all reactions were carried out in heat-gun dried glassware under an inert gas atmosphere (nitrogen, argon) using standard Schlenk techniques. All chemicals and solvents were purchased from Acros, Sigma-Aldrich, fluorochem or abcr GmbH. 1,4-Diiodobenzene was purchased from Sigma-Aldrich and purified by column chromatography before use. THF and toluene were dried employing a MB SPS-800 solvent purification system with drying

columns. Deuterated solvents were obtained from Sigma-Aldrich. NMR spectra were recorded in deuterated solvents at room temperature on a Bruker Avance 300 (300 MHz), a Bruker Avance 500 (500 MHz) or a Bruker Avance III (600 MHz) spectrometer. Emission and excitation spectra were recorded on a Jasco FP 6500. Samples were prepared as suspensions in THF (*c* = 1 mg/mL). UV-Vis solid state spectra were recorded using a spectrometer equipped with an integration sphere (Photon Technology International Quantummaster 40, LabSphere®; diameter 6", coated with Spectrafect®). The bandwidths of the monochromator were set to 3 nm (incident light and reflected light). As a white standard we used magnesium sulfate (reflected light). Thermogravimetric analyses were performed using a Mettler Toledo TGA/DSC1 device. Porosity of the polymers was characterized by nitrogen BET analysis at 77.35 K with an autosorb computer controlled surface analyzer (AUTOSORB-iQ 3, Quantachrome). The sample was degassed at 80 °C (3 h) before analysed. The Brunauer-Emmett-Teller (BET) surface area was calculated assuming a value of 0.162 nm<sup>2</sup> for the cross sectional area of the nitrogen molecules in the pressure range *P*/*P*<sub>0</sub> = 0.01-0.1. IR spectra were recorded on a Jasco FT/IR-4100 spectrometer. Substances were applied as solids. Infrared data are quoted in wave numbers [cm<sup>-1</sup>]. Elemental Analysis was performed by the Microanalytical Laboratory of the University of Heidelberg using an Elementar Vario EL machine. Photographs were taken with a Canon EOS 7D camera. Lifetime estimation of excited states after fluorescence stimulation was accomplished with a Horiba Yvon Fluorocube at different wavelengths.

**Monomer synthesis. General Procedure (GP) 1** for the synthesis of tetra(4-bromophenyl)-compounds **2-4** via lithiation. 1,4-Dibromobenzene (1.0 eq) is dissolved in diethyl ether. The solution is cooled to 0 °C and *n*-butyl lithium (1.0 eq, 2.5 M in hexane) is added dropwise. The mixture is stirred for 30 min at this temperature. Then, MCl<sub>4</sub> (0.25 eq., M = Si, Ge, Sn) is added dropwise. The mixture is stirred overnight and allowed to warm to room temperature during this time. DI water is added to quench the reaction and dichloromethane is added until all residues are dissolved. The phases are separated and the aqueous layer is extracted with dichloromethane. The combined organic layers are dried over MgSO<sub>4</sub>, the solvent evaporated and the remaining, off-white solid recrystallized from ethyl acetate. See Supporting Information for analytical data of **1-4**.

**GP2** for the Sonogashira coupling of group IV-tetra(4-bromophenyl)-compounds **1-4** with trimethylsilyl-acetylene. The respective group IV-aryl bromide (1.0 eq) is dissolved in a degassed 1:1 mixture of tetrahydrofuran/diisopropylamine. CuI (0.10 eq), tris(*tert*-butyl)-phosphonium tetrafluoroborate (0.20 eq.), trimethylsilyl acetylene (10 eq) and bisbenzotriledichloro palladium(II) (0.10 eq) are added in this order. The mixture is stirred for 3 days at room temperature and then quenched by addition of DI water. The aqueous phase is extracted with dichloromethane. The combined organic layers are dried over MgSO<sub>4</sub>, filtered and the solvent evaporated. The remaining, dark brown solid is dissolved in a 2:1 mixture petroleum ether/dichloromethane and filtered through a silica plug. After removal of the solvent, the remaining off-white solid is recrystallized from ethyl acetate to yield the crystalline trimethylsilyl protected tetraalkyne. See Supporting Information for analytical data of **5-8**.

**GP3** for the desilylation of trimethylsilyl protected tetraalkynes **5-8**. The respective trimethylsilyl protected alkyne (1.0 eq) is dissolved in a mixture of tetrahydrofuran/methanol. K<sub>2</sub>CO<sub>3</sub> (20 eq) is added and the suspension is stirred at room temperature. The reaction is quenched by addition of DI water and the aqueous phase extracted with dichloromethane. The combined organic layers are dried over MgSO<sub>4</sub>, the solvent evaporated and the residual off-white solid recrystallized from hexane and ethyl acetate to yield the respective terminal alkynes. See Supporting Information for analytical data of **9-12**.

## FULL PAPER

**Polymer synthesis. GP4 for CMPs C-1 – Sn-1:** The respective tetrahedral monomer (1.0 eq) was dissolved in a degassed mixture of toluene and triethylamine. Then, 1,4-diiodobenzene (2.0 eq) and bis(triphenylphosphine)palladium(II) dichloride (2 mol%) were added. The reaction mixture was stirred at 100 °C overnight and filtered. The solid was pestled in a mortar, washed with methanol and subjected to Soxhlet extraction from methanol overnight. The resulting powder was pestled in a mortar again and dried *in vacuo* to yield the respective polymer. See Supporting Information for analytical data of **C-1 – Sn-1**.

**GP5 for CMPs C-2 – Sn-2:** The respective tetrahedral monomer (1.0 eq) was dissolved in a degassed mixture of DMF and triethylamine. Then, 1,4-diiodobenzene (2.0 eq) and tetrakis(triphenylphosphine)palladium(0) (2 mol%) were added. The reaction mixture was stirred at 100 °C overnight and filtered. The solid was pestled in a mortar, washed with methanol and subjected to Soxhlet extraction from methanol overnight. The resulting powder was pestled in a mortar again and dried *in vacuo* to yield the respective polymer. See Supporting Information for analytical data of **C-2 – Sn-2**.

**GP6 for CMPs C-3 – Sn-3:** The respective tetrahedral monomer (1.0 eq) was dissolved in a degassed mixture of THF and DIPA. 1,4-Dibromobenzene (2.0 eq), CuI (4 mol%), HP(*t*Bu)<sub>3</sub>BF<sub>4</sub> (4 mol%) and Pd(PhCN)<sub>2</sub>Cl<sub>2</sub> (2 mol%) were added. The reaction mixture was stirred at 40 °C for 3 d and filtered. The solid was pestled in a mortar, washed with methanol and subjected to Soxhlet extraction from methanol overnight. The resulting powder was pestled in a mortar again and dried *in vacuo* to yield the respective polymer. See Supporting Information for analytical data of **C-3 – Sn-3**.

## Acknowledgements

We thank Prof. M. Mastalerz and Sven Elbert for sorption analysis instrument time and supportive discussions. F. L. Geyer expresses his gratitude to the German National Academic Foundation (Studienstiftung) for receiving a PhD scholarship.

**Keywords:** tetrahedral connectors • microporous polymers • 3D networks • structure-property-relationship

- [1] J. B. Lambert, Z. Liu, C. Liu, *Organometallics* **2008**, *27*, 1464-1469.
- [2] M. Mastalerz, H.-J. S. Hauswald, R. Stoll, *Chemical Communications* **2012**, *48*, 130-132.
- [3] T. Ben, H. Ren, S. Ma, D. Cao, J. Lan, X. Jing, W. Wang, J. Xu, F. Deng, J. M. Simmons, S. Qiu, G. Zhu, *Angewandte Chemie* **2009**, *121*, 9621-9624.
- [4] A. P. Côté, H. M. El-Kaderi, H. Furukawa, J. R. Hunt, O. M. Yaghi, *Journal of the American Chemical Society* **2007**, *129*, 12914-12915.
- [5] D. Beaudoin, T. Maris, J. D. Wuest, *Nature Chemistry* **2013**, *5*, 830.
- [6] F. J. Uribe-Romo, J. R. Hunt, H. Furukawa, C. Klöck, M. O’Keeffe, O. M. Yaghi, *Journal of the American Chemical Society* **2009**, *131*, 4570-4571.
- [7] J.-X. Jiang, F. Su, A. Trewin, C. D. Wood, N. L. Campbell, H. Niu, C. Dickinson, A. Y. Ganin, M. J. Rosseinsky, Y. Z. Khimyak, A. I. Cooper, *Angewandte Chemie International Edition* **2007**, *46*, 8574-8578.
- [8] L. Chen, Y. Honsho, S. Seki, D. Jiang, *Journal of the American Chemical Society* **2010**, *132*, 6742-6748.
- [9] U. H. F. Bunz, K. Seehafer, F. L. Geyer, M. Bender, I. Braun, E. Smarsly, J. Freudenberg, *Macromolecular Rapid Communications* **2014**, *35*, 1466-1496.
- [10] X. Liu, Y. Xu, D. Jiang, *Journal of the American Chemical Society* **2012**, *134*, 8738-8741.
- [11] J. R. Holst, E. Stöckel, D. J. Adams, A. I. Cooper, *Macromolecules* **2010**, *43*, 8531-8538.
- [12] J. Liu, J. M. Tobin, Z. Xu, F. Vilela, *Polymer Chemistry* **2015**, *6*, 7251-7255.
- [13] R. Dawson, A. Laybourn, R. Clowes, Y. Z. Khimyak, D. J. Adams, A. I. Cooper, *Macromolecules* **2009**, *42*, 8809-8816.
- [14] X. Zhuang, D. Gehrig, N. Forler, H. Liang, M. Wagner, M. R. Hansen, F. Laquai, F. Zhang, X. Feng, *Advanced Materials* **2015**, *27*, 3789-3796.
- [15] Y. Zhu, H. Yang, Y. Jin, W. Zhang, *Chemistry of Materials* **2013**, *25*, 3718-3723.
- [16] R. K. Totten, M. H. Weston, J. K. Park, O. K. Farha, J. T. Hupp, S. T. Nguyen, *ACS Catalysis* **2013**, *3*, 1454-1459.
- [17] D. Yuan, W. Lu, D. Zhao, H.-C. Zhou, *Advanced Materials* **2011**, *23*, 3723-3725.
- [18] E. Stockel, X. Wu, A. Trewin, C. D. Wood, R. Clowes, N. L. Campbell, J. T. A. Jones, Y. Z. Khimyak, D. J. Adams, A. I. Cooper, *Chemical Communications* **2009**, 212-214.
- [19] L. Monnereau, T. Muller, M. Lang, S. Brase, *Chemical Communications* **2016**, *52*, 571-574.
- [20] Z.-Z. Yang, Y. Zhao, H. Zhang, B. Yu, Z. Ma, G. Ji, Z. Liu, *Chemical Communications* **2014**, *50*, 13910-13913.
- [21] B. Kim, N. Park, S. M. Lee, H. J. Kim, S. U. Son, *Polymer Chemistry* **2015**, *6*, 7363-7367.
- [22] A. C. Uptmoor, R. Ilyas, S. M. Elbert, I. Wacker, R. R. Schröder, M. Mastalerz, J. Freudenberg, U. H. F. Bunz, *Chemistry – A European Journal*, n/a-n/a.
- [23] J.-H. Fournier, W. Xin, J. D. Wuest, *Canadian Journal of Chemistry* **2003**, *81*, 376.
- [24] P. Li, Y. He, H. D. Arman, R. Krishna, H. Wang, L. Weng, B. Chen, *Chemical Communications* **2014**, *50*, 13081-13084.
- [25] M. Wander, P. J. C. Hausoul, L. A. J. M. Sliedregt, B. J. van Steen, G. van Koten, R. J. M. Klein Gebbink, *Organometallics* **2009**, *28*, 4406-4415.
- [26] A. C. Uptmoor, J. Freudenberg, S. T. Schwäbel, F. Paulus, F. Rominger, F. Hinkel, U. H. F. Bunz, *Angewandte Chemie International Edition* **2015**, *54*, 14673-14676.
- [27] T. Hundertmark, A. F. Littke, S. L. Buchwald, G. C. Fu, *Organic Letters* **2000**, *2*, 1729-1731.
- [28] F. L. Geyer, F. Rominger, M. Vogtland, U. H. F. Bunz, *Crystal Growth & Design* **2015**, *15*, 3539-3544.
- [29] E. Galoppini, R. Gilardi, *Chemical Communications* **1999**, 173-174.

## FULL PAPER

- [30] H. Ma, H. Ren, X. Zou, F. Sun, Z. Yan, K. Cai, D. Wang, G. Zhu, *Journal of Materials Chemistry A* **2013**, *1*, 752-758.
- [31] M. Trunk, A. Herrmann, H. Bildirir, A. Yassin, J. Schmidt, A. Thomas, *Chemistry – A European Journal* **2016**, *22*, 7179-7183.
- [32] Z.-Q. Chen, T. Chen, J.-X. Liu, G.-F. Zhang, C. Li, W.-L. Gong, Z.-J. Xiong, N.-H. Xie, B. Z. Tang, M.-Q. Zhu, *Macromolecules* **2015**, *48*, 7823-7835.
- [33] L. Pu, *Macromolecular Rapid Communications* **2000**, *21*, 795-809.
- [34] H. Yamagata, F. C. Spano, *The Journal of Physical Chemistry Letters* **2014**, *5*, 622-632.
- [35] M. Moroni, J. Le Moigne, S. Luzzati, *Macromolecules* **1994**, *27*, 562-571.
- [36] N. B. Shustova, A. F. Cozzolino, S. Reineke, M. Baldo, M. Dincă, *Journal of the American Chemical Society* **2013**, *135*, 13326-13329.
- [37] R. Haldar, A. Mazel, R. Joseph, M. Adams, I. A. Howard, B. S. Richards, M. Tsotsalas, E. Redel, S. Diring, F. Odobel, C. Wöll, *Chemistry – A European Journal* **2017**, *23*, 14316-14322.
- [38] Z. Hu, T. Adachi, R. Haws, B. Shuang, R. J. Ono, C. W. Bielawski, C. F. Landes, P. J. Rossky, D. A. Vanden Bout, *Journal of the American Chemical Society* **2014**, *136*, 16023-16031.
- [39] R. Dawson, A. Laybourn, Y. Z. Khimyak, D. J. Adams, A. I. Cooper, *Macromolecules* **2010**, *43*, 8524-8530.

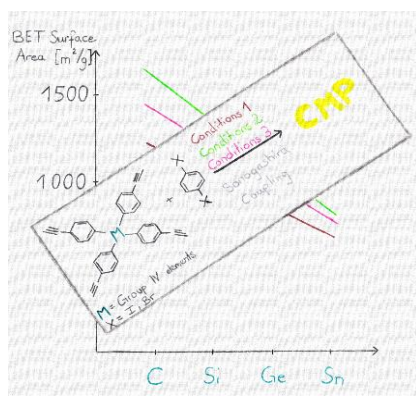
## FULL PAPER

## Entry for the Table of Contents (Please choose one layout)

Layout 1:

## FULL PAPER

**The center makes a difference:** A comparison of microporous polymers with group IV (tetra(*p*-ethynylphenyl) monomers reveals the same trend for the central atom-dependent surface areas independent from the Sonogashira-Hagihara polymerization protocol employed.



Andrea C. Uptmoor, Florian L. Geyer,  
Frank Rominger, Jan Freudenberg\* and  
Uwe H. F. Bunz\*

Page No. – Page No.

**Tetrahedral Tetrakis(*p*-ethynylphenyl)-Group IV-Compounds in Microporous Polymers: Effect of Tetrel on Porosity**

Layout 2:

## FULL PAPER

((Insert TOC Graphic here; max. width: 11.5 cm; max. height: 2.5 cm))

Author(s), Corresponding Author(s)\*

Page No. – Page No.

Title

Text for Table of Contents